PAPER • OPEN ACCESS

Q-switched pulse generation in L-band region with polyacrylonitrile saturable absorber

To cite this article: Aeriyn D Ahmad *et al* 2024 *Phys. Scr.* **99** 065562

Physica Scripta

PAPER

Q-switched pulse generation in L-band region with polyacrylonitrile saturable absorber

Aeriyn D Ahmad[1], **Sameer Salam**[2], **Norrima Mokhtar**[1], **Hamzah Arof**[1], **Retna Apsari**[3], **Belal Ahmed Hamida**[4] and **Sulaiman W Harun**[1,3,*]

[1] Photonics Engineering Laboratory, Department of Electrical Engineering, University of Malaya, 50603 Kuala Lumpur, Malaysia
[2] Department of Communications Technology Engineering, Technical College, Imam Ja'afar Al-Sadiq University, Baghdad, Iraq
[3] Department of Physics, Faculty of Science and Technology, Airlangga University, Surabaya, Indonesia
[4] Department of Electrical and Computer Engineering, Kulliyah of Engineering, International Islamic University of Malaysia, Gombak, Selangor, Malaysia
[*] Author to whom any correspondence should be addressed.

E-mail: aeriyndwierni@gmail.com **and** swharun@um.edu.my

Keywords: polyacrylonitrile, Q-switched laser, L-band, EDFL, thin film

OPEN ACCESS

RECEIVED
3 April 2024

REVISED
22 April 2024

ACCEPTED FOR PUBLICATION
17 May 2024

PUBLISHED
28 May 2024

Abstract

In this study, we assess the practicality of using Polyacrylonitrile (PAN) as a saturable absorber (SA) for generating Q-switched pulses within an erbium-doped fibre laser (EDFL) cavity. A successful combination of PAN, a resin material, and polyvinyl alcohol resulted in the formation of a SA film. This film was utilised to generate stable Q-switched pulses operating in a long-wavelength band of 1572 nm. The greatest repetition rate achieved was 66.1 kHz, while the minimum pulse width was 2.43 μs. The maximum pulse energy was achieved at 52 nJ and measured at a pump power of 175.9 mW. To the best of our knowledge, this study is the first report of EDFL passive Q-switching employing a PAN absorber.

Introduction

The Fourth Industrial Revolution (4IR), characterized by the integration of digital technologies into various industries, demands advanced laser technologies for precise and efficient material processing. Q-switched fiber lasers have emerged as a promising tool in this context, offering high power, excellent beam quality, fast pulse generation capabilities and wide-ranging applications such as micro-machining [1], imaging [2], medical applications [3] and telecommunications [4]. Q-switched fiber lasers have also shown important potential in laser machining and additive manufacturing processes. Rung *et al* [5] investigates the use of Q-switched fiber lasers for micro-machining of metals with high precision and minimal heat-affected zones. Additionally, studies by Chaudhary *et al* [6] explore the application of Q-switched fiber lasers in additive manufacturing, enabling rapid prototyping and production of complex parts. The previous reports also have shown that Q-switched fiber lasers have demonstrated their effectiveness in laser cutting and welding applications. Chen *et al* [7] presents a study on high-power Q-switched fiber lasers for efficient and precise cutting of thin metal sheets. Furthermore, studies by Saunders *et al* [8] explore the use of Q-switched fiber lasers for laser welding of dissimilar materials, offering excellent weld quality and control.

Several Q-switching techniques are employed in fiber lasers, including acoustic-optic modulation (AOM), electro-optic modulation (EOM), and saturable absorber (SA). Previously, Qamar *et al* [9] and Tang *et al* [10] explore the principles and performance of these techniques, highlighting their advantages and limitations. Previously, the generation of Q-switched pulses relied on active methods like AOMs [11, 12] or EOMs [13, 14]. However, these approaches face limitations due to their bulky nature, complex operation, and costly fabrication processes [15, 16]. Consequently, passive Q-switching has emerged as a preferred, cost-effective alternative to active methods, typically achieved through a saturable absorber (SA). SAs are commonly employed in fiber laser systems for generating Q-switched and mode-locked lasers [17–19]. Previous studies have demonstrated that Q-switching and mode-locking lasers can also be achieved using a nonlinear polarization rotation technique

(NPR) [20, 21]. In this context, various types of SAs have been investigated for their efficacy in producing high-performance Q-switched pulses, including semiconductor SA mirrors (SESAMs) [22], graphene [23, 24], carbon nanotubes (CNTs) [25, 26], topological insulators (TIs) [27, 28], black phosphorus (BP) [29, 30], transition metal oxides (TMOs) [31, 32], and transition metal dichalcogenides (TMDs) [33].

Recently, many interests have also been focused on Polyacrylonitrile (PAN) material due to its exceptional electrical and mechanical properties, as well as its chemical resistance and thermal stability. PAN is a synthetic polymer derived from the monomer acrylonitrile, and it is structurally composed of a linear polymer featuring repeating units of acrylonitrile monomers. This organic polymer exhibits a semicrystalline nature and is characterized by the chemical formula $[C_3H_3N]_n$, with a nitrile (CN) functional group attached to its polyethylene backbone as the fundamental unit structure. The nitrile group, acting as a hydrogen bonding acceptor, possesses a large dipole moment between the electron-deficient carbon atom and the electron-rich nitrogen atom, facilitating relatively strong attractive interactions. Consequently, these strong intermolecular interactions contribute to the polymer's high strength and resistance to various organic solvents [34]. Such properties render PAN highly desirable for the development of high-performance composites in automotive and aerospace technologies, owing to its enhanced physical and mechanical characteristics. Scholars such as Fitzer [35], Chen and Harrison [36, 37] have suggested that optimizing PAN fiber could ideally result in high-performance materials suitable for aerospace applications. Here, we explore the application of PAN material in fiber laser as a SA.

This paper presents the demonstration of a passively Q-switched erbium-doped fiber laser (EDFL) utilizing a newly developed PAN film as a SA for operation within the L-band region. The PAN film SA, fabricated via a casting approach, was placed between two FC/PC ferrules to generate Q-switched laser pulses at a central wavelength of 1572.0 nm. The highest repetition rate and the lowest pulse width achieved was 66.1 kHz and 2.43 μs, respectively. Notably, this study marks the first successful implementation of a PAN film as an SA in an EDFL operating at L-band region. The proposed PAN film is easier to incorporate into all-fiber geometries and cheaper compared to other passive Q-switchers, such as semiconductor saturable absorber mirrors [38].

Preparation and characterization of PAN SA

In this study, PAN material serves as the SA, facilitating Q-switching by modulating the cavity loss. This choice is motivated by its numerous advantages, including straightforward synthesis, robust conductivity, and cost-effectiveness. The PAN powder used as the raw material, obtained from Macklin Biochemical Technology, appears as a white to yellow powder with the chemical formula $(C_3H_3N)_n$. Polyvinyl Alcohol (PVA) serves as the host polymer due to its excellent film-forming properties, ease of emulsification, high tensile strength, and high-water solubility. Additionally, it demonstrates minimal absorption of white light and boasts a high melting temperature of 200 °C, rendering it ideal for high-intensity laser applications. The fabrication process is not only cost-effective but also hazard-free. The fabrication of the PAN-PVA film follows a drop-and-casting procedure. Initially, 1 g of PVA powder is dissolved in 120 ml of distilled water and stirred for three hours to prepare a homogeneous PVA solution. Subsequently, 8 mg of PAN powder is added to 10 ml of the prepared PVA solution, and the mixture is stirred for approximately three days. Following this, 5 ml of the thoroughly mixed PAN-PVA solution is delicately applied onto a 3.5 cm diameter petri dish. The dish is then left to dry for approximately three days, resulting in a thin film with an estimated thickness of 50 μm. Figure 1(a) illustrates the step-by-step preparation process.

The elemental composition and physical characteristics of the PAN-PVA thin film were analysed using Energy Dispersive x-ray Spectroscopy (EDX) and Field Emission Electron Microscopy (FESEM), respectively. The EDX analysis (depicted in figure 1(b)) probed into the elemental makeup of the film, revealing a predominant presence of carbon (C), nitrogen (N), and oxygen (O), with the oxygen component primarily originating from the PVA matrix. Figure 1(c) presents the FESEM image, indicating a uniform surface morphology of the PAN-PVA thin film and demonstrating a well-dispersed distribution of PAN particles within the PVA matrix. This uniformity significantly enhances the film's efficacy as a SA material.

The linear absorption characteristics of the SA were determined by illuminating the thin film with a broadband light source emitted from a white light source and measuring the output using an optical spectrum analyser (OSA). The results, presented in figure 2(a), indicated an absorption of 0.74 dB at a wavelength region of 1570 nm. For the evaluation of nonlinear absorption, a balanced twin-detector system (illustrated in the inset of figure 2(b)) was employed [39]. A mode-locked fiber laser, operating at a center wavelength of 1567 nm with a pulse width of 700 fs and a repetition rate of 21.73 MHz, served as the primary laser source. The laser output intensity was regulated by passing through an optical amplifier a[illegible]ble optical attenuator (VOA). The beam power was then equally divided into two portions by a 3 d[illegible] One portion acted as a reference

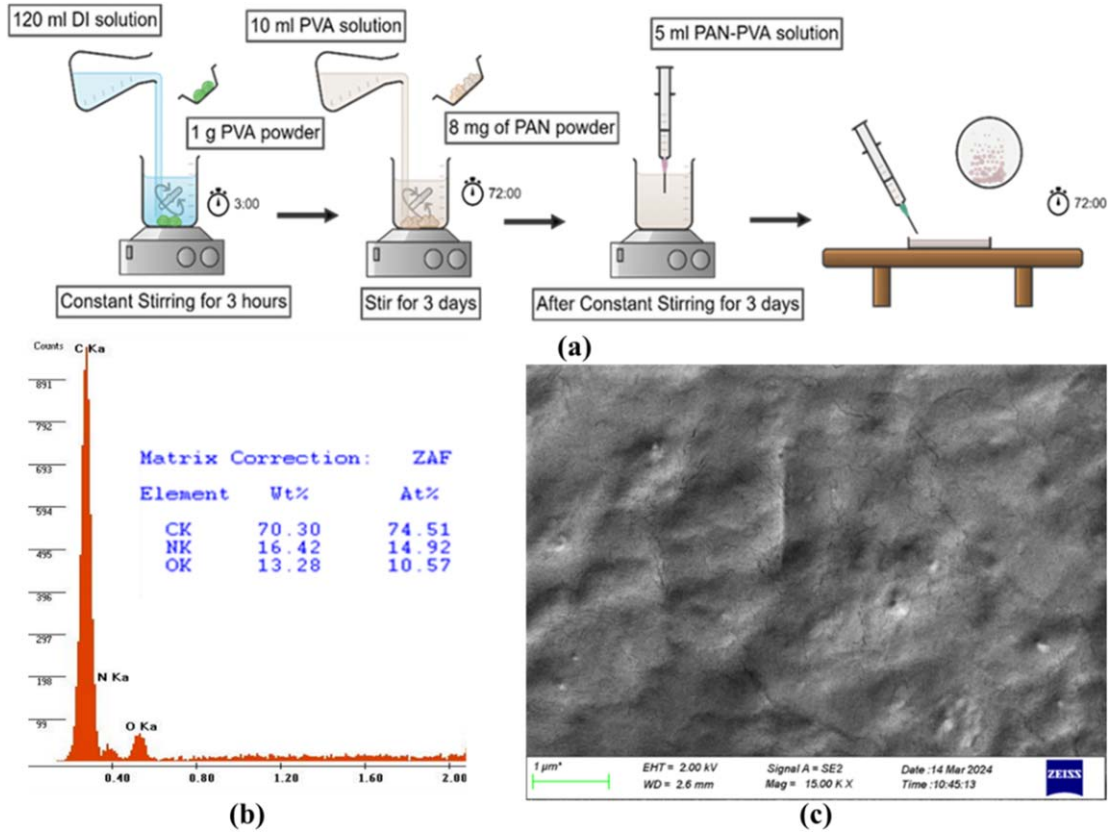

Figure 1. (a) Step by step procedure fabricating PAN-PVA film, (b) EDX analysis result, and (c) The FESEM image at 15000 times magnification.

power, directly connected to an optical power meter, while the other passed through the PAN SA, and the transmitted power was recorded by another optical power meter.

The nonlinear absorption curve was fitted using the equation [40]:

$$\alpha(I) = \frac{\alpha_0}{\left(1 + \frac{I}{I_{sat}}\right)} + \alpha_{ns}$$

where α_0, I_{sat}, and α_{ns}, represent the saturable absorption, saturation intensity, and non-saturable absorption, respectively. $\alpha(I)$ denotes the total intensity-dependent absorption coefficient. Experimental results depicted in figure 2(b) revealed $\alpha_0 = 11.4\%$, $I_{\text{sat}} = 20$ MW cm^{-2}, and $\alpha_{ns} = 45\%$. These findings indicate that the absorption properties of the PAN SA undergo changes with incident light intensity. At low intensities, the device permits high transmission, but as intensity rises, absorption saturates, resulting in reduced transmission. This characteristic can be utilized to modulate the laser's cavity loss for Q-switching. However, the SA displays a notable non-saturable loss of approximately 45%. This characteristic contributes to an elevation in the threshold pump power needed to trigger the switching process. Enhancing the performance of the laser system, particularly in terms of Q-switching threshold and overall efficiency, may be achievable through additional optimization of SA fabrication to minimize the non-saturable loss component.

Laser configuration

A ring EDFL setup was constructed to evaluate the performance of PAN film, as illustrated in figure 3. The laser cavity comprises a 0.7 m long EDF with an absorption coefficient of 68 dB m^{-1} at 980 nm, a polarization-independent isolator, a PAN-based SA, a 10 dB fiber-fused coupler, and a wavelength-division multiplexer (WDM). A 980 nm laser diode pumps the EDF via the WDM. An optical isolator positioned between the EDF, and the SA device ensures unidirectional propagation of light within the cavity. The laser output is extracted from the cavity through a 90:10 output coupler, which permits only 10% of the output to be collected for analysis. The PAN-based SA device is assembled by placing the fabricated film between two FC/PC fiber ferrules and then inserted into the laser cavity. The insertion loss of the P easures approximately 1.4 dB, reflecting its inherently low level, which is conducive to efficien ation. This minimal loss permits a

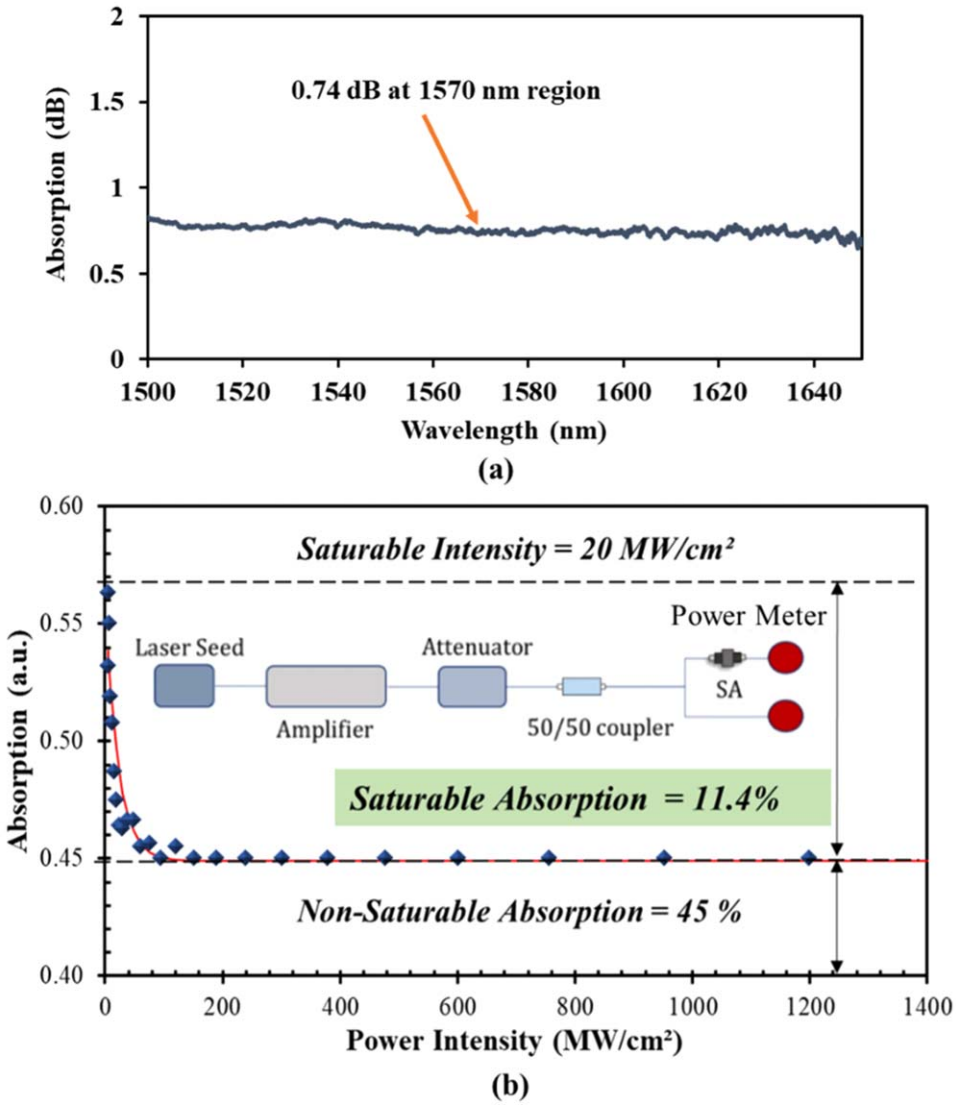

Figure 2. (a) The linear absorption spectrum (b) nonlinear absorption profile. Inset shows the configuration of a balanced twin-detector system.

greater portion of laser light to transmit through the device, facilitating optimal Q-switching performance. The total length of the cavity measures approximately 14 m. Typically, shorter cavity lengths correlate with shorter pulse durations in Q-switched fiber lasers. However, other factors such as the characteristics of the gain fiber, dispersion, and SA can also significantly impact pulse duration. For instance, shorter gain fiber may reach saturation more rapidly, resulting in shorter pulses. To characterize the spectral properties of the output laser, an optical spectrum analyzer (ANRITSU, MS9710C) is employed, while optical power is measured using a power meter (THORLABS, PM310D). Analysis of the temporal behaviour of the generated Q-switched pulses is conducted utilizing a 350 MHz digital storage oscilloscope (GWINSTEK, GDS-3352) and a 7.8 GHz radio frequency (RF) spectrum analyzer (ANRITSU, MS2683A) in conjunction with a 7-GHz InGaAs photodetector.

Results and discussion

The PAN-PVA film was first taken out of the laser cavity so that the performance of self-mode-locking or self-Q-switching in the EDFL cavity without the PAN-PVA SA could be studied. Despite the vast range of pump power variations, only a continuous-wave (CW) laser was obtained. The CW laser was first seen working with a pumping power of 80 mW after the PAN-PVA film was put into the EDFL cavity using a sandwich-structured fiber-ferrule platform. Subsequently, steady Q-switched laser pulses were recorded as the pump power was increased to 113.3 mW and the Q-switching operation remained with the further increase of pump power up to 175.9 mW. The passive Q-switching relies on the PAN film's abi dulate the loss within the laser cavity in response to changes in light intensity. Initially, the PAN SA abs ausing a high loss in the cavity, which

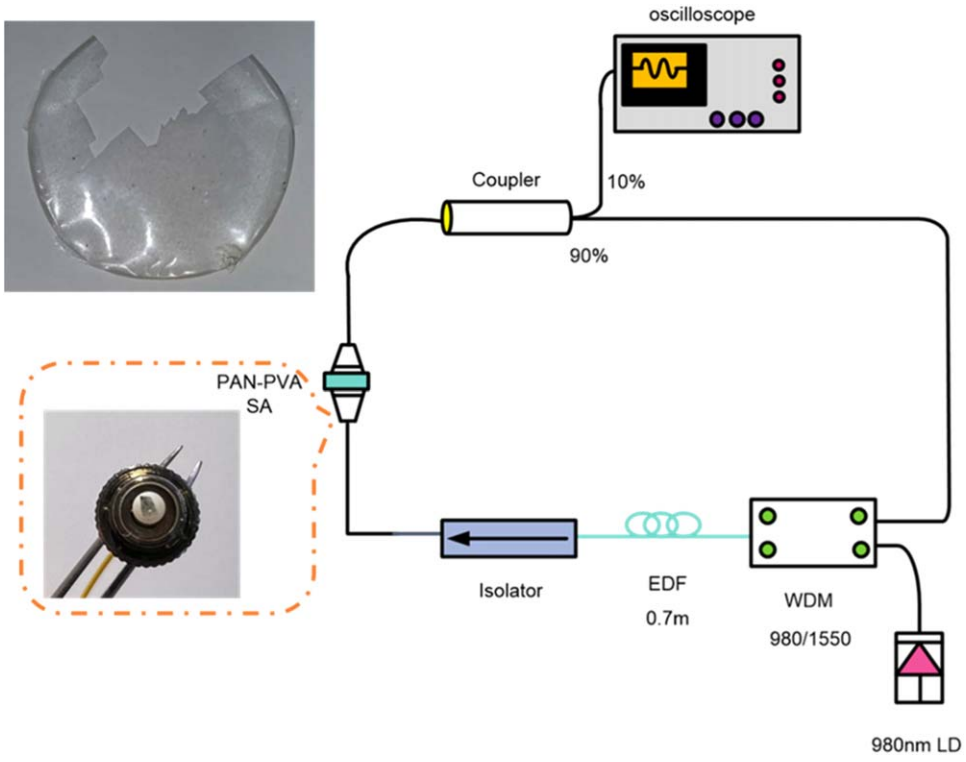

Figure 3. Schematic of the Q-switched EDFL setup featuring a PAN-PVA SA. Inset highlights a visual depiction of the PAN-PVA thin film, affixed to a fiber ferrule tip, utilized in SA device construction.

prevents laser action. However, as the intensity of the light pulses increases, the SA saturates and becomes transparent, reducing the loss in the cavity. This mechanism enables the generation of Q-switched pulses with precise control over pulse duration and repetition rate. Figure 4(a) displays the pulse trains of the Q-switched laser at three distinct pump powers. The pulse output exhibited uniform and stable pulse train as the pump power varied between 113.27 mW and 175.9 mW, while the pulse-to-pulse interval decreased from 20.3 to 15.1 μs. The repetition rate and pulse width patterns exhibit conformity with the characteristic attributes commonly observed in Q-switched fiber lasers. The pulses also exhibited minimal amplitude modulation, indicating the lack of self-mode-locking effects on Q-switching.

Figures 4(b) and (c) depict the optical and radio frequency (RF) spectra obtained at a power level of 175.9 mW for the diode. The Q-switched pulses were observed to function at a central wavelength of 1572.0 nm, as depicted in figure 4(b). The RF spectrum exhibits numerous harmonics, with the primary frequency observed at 66.1 kHz. The signal-to-noise ratio (SNR) of the RF signal at this frequency surpassed 50 dB, providing more evidence to support the stability of the Q-switching operation. Furthermore, it's crucial to acknowledge that the proposed laser setup did not include a polarization controller because polarization had negligible impact on the laser and pulsing activities. It was noted that modifying the polarization state of the cavity had minimal impact on the properties of the optical spectrum and pulse trains. It's also important to note that, in the current experiment, only Q-switched pulses can be generated within the cavity setup. However, extending the cavity length to incorporate dispersion management holds the promise of transitioning to a mode-locked pulse train. This adjustment facilitates pulse formation, enhances nonlinear effects, and offers external control—essential elements for attaining stable and efficient mode-locking.

Figure 5 illustrates the attributes of the laser pulses in relation to the power of the pump. Figure 5(a) depicts the relationship between the average output power, the single pulse energy, and the pump power. The Q-switched functioning remained constant while the pump power increased from 113.3 mW to 175.9 mW, while the average output power exhibited a virtually linear growth from 0.7 to 3.47 mW. The increase in pump power will result in a greater gain, hence generating a higher pulse energy because of the accelerated accumulation of Q-switched pulse. The energy of a single pulse can reach a maximum of 52 nJ. Figure 5(b) illustrates the relationship between the pulse repetition rate and width as pump power increases. For the mode-locked fiber laser, the repetition rate stays the same no matter how long the cavity is. But for Q-switched pulses, the generation rate changes based on how saturated the surface area (SA) is. Hence, there exists a positive correlation between the repetition rate of the laser and the pump[illegible]s depicted in figure 5(b). The frequency increased from 50.0 to 66.1 kHz in conjunction with the corresp[illegible]crease in pump power from 113.3 to

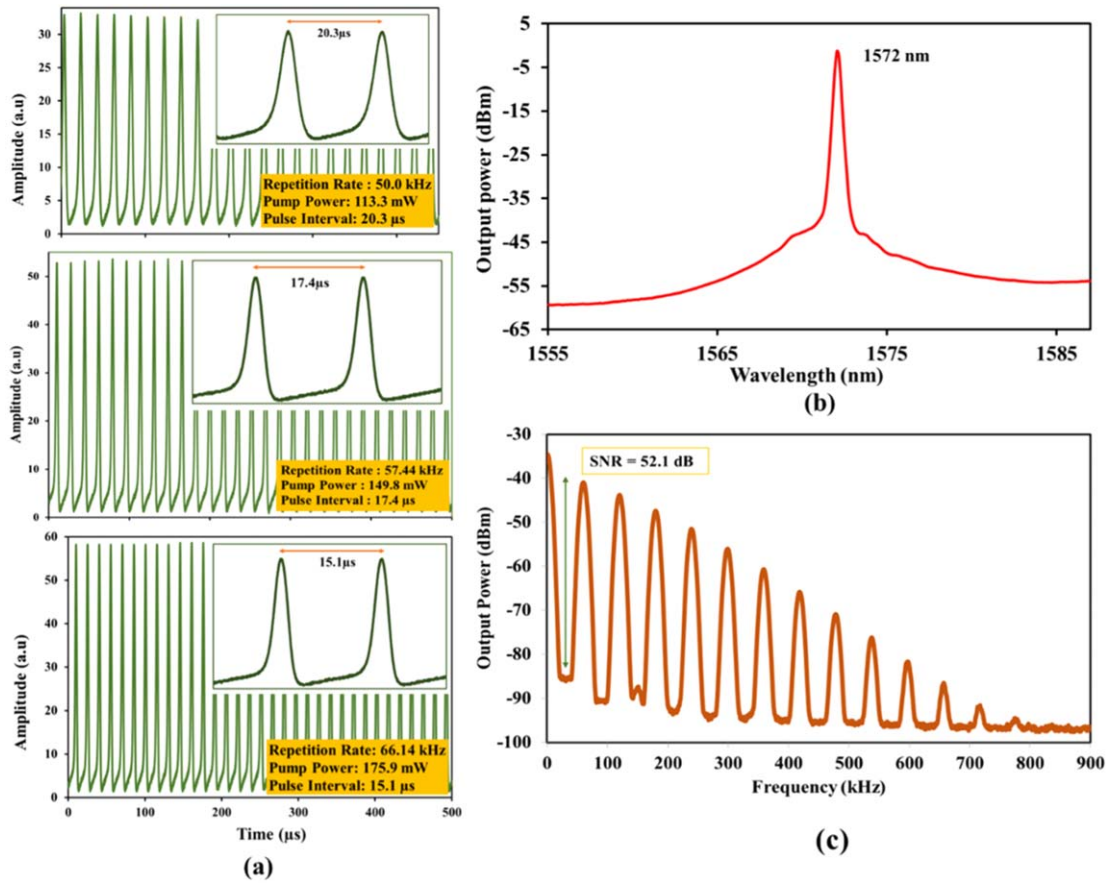

Figure 4. Temporal, spectral and frequency characteristics of the laser (a) typical oscilloscope trace at pump powers of 113.3, 149.8 and 175.9 mW (b) output spectrum, and (c) RF spectrum with initial span of 900 kHz.

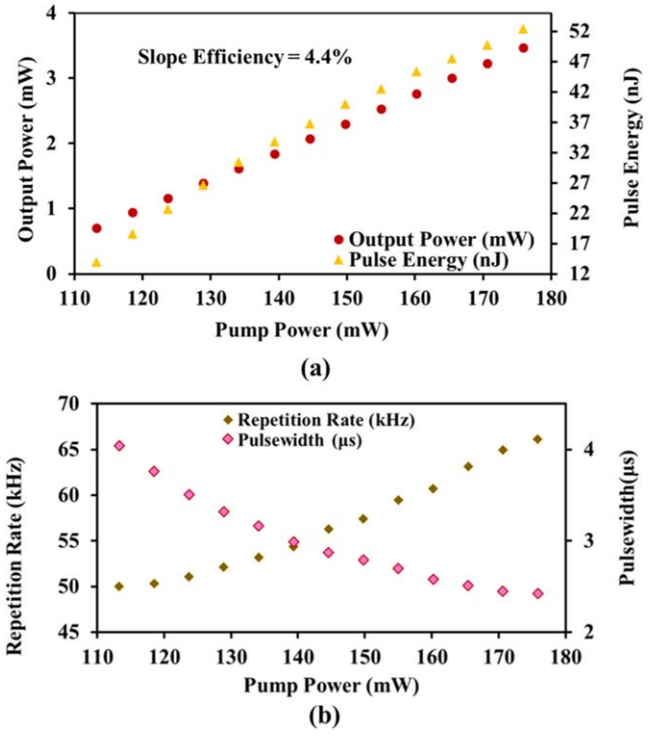

Figure 5. The Q-switched laser performances against the input pump power (a) Output power and pulse energy, (b) repetition rate and pulse width.

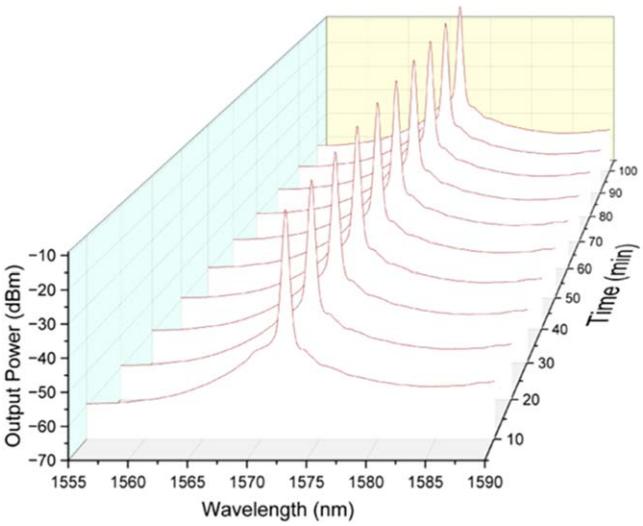

Figure 6. Output spectra of the Q-switched pulses monitored over 100 min.

Table 1. Comparative analysis of multiple reported Q-switched EDFLs utilizing different SAs.

SA materials	Modulation depth (%)	Wavelength (nm)	Max. repetition rate (kHz)	Min. pulse width (μs)	Max. pulse energy (nJ)	References
Graphene	NA	1522 ~ 1555	103	2	40	[41]
Bi_2Te_3	4.1	1558.1	47.1	1.58	17.8	[42]
$MoSe_2$	NA	1562.3	32.8	30.4	57.9	[43]
WSe_2	3.5	1560	49.6	3.1	33.2	[44]
WS_2	2.1	1560	39.37	3.71	126.96	[45]
Bi_2Se_3	39.8	1560	68.2	2.4	47.1	[46]
V_2AlC	NA	1559	53.55	2.54	57.14	[47]
MoAIB	10.4	1559	82.92	2.14	27.49	[48]
PAN	11.4	1572.0	66.1	2.43	52	This work

175.9 mW. The increase in repetition rate is attributed to the SA mechanism, which exhibits a greater saturation rate when subjected to higher pump power. In contrast, there was a drop in pulse width from 4.04 to 2.43 μs as the pump power increased from 113.3 to 175.9 mW. Apart of the slope efficiency measured at 4.4%, the augmentation of pump power leads to an elevation in the rate of photon density growth, which serves as a measure of the duration of energy storage. Consequently, the formation of quicker pulses occurs, leading to an increased repetition rate. However, as the pump power surpasses 175.9 mW, we observed instability in the generated pulses. This instability arises from a combination of saturation effects in both the SA and the gain medium, mode competition, and thermal effects within the laser cavity.

To thoroughly assess the stability of the Q-switched EDFL, its output spectra were monitored over consecutive 10 min intervals, totaling 100 min of observation. The experimental result is illustrated in figure 6, which indicates the exceptional stability of the proposed Q-switched fiber laser, demonstrating consistent performance over prolonged periods. Operating consistently at a wavelength of 1572.0 nm, the spectral characteristics remained resolutely unchanged throughout the observation period, with peak intensity fluctuations meticulously maintained within a narrow margin of $\pm$ 0.1 dB. Additionally, extensive monitoring via oscilloscope traces spanning three days reaffirmed the robustness of the pulse trains. Notably, the absence of fluctuations or noise underscored the enduring stability of the laser's operation. The performance of the proposed PAN-based Q-switched fiber laser was compared with that of recently reported passively Q-switched EDFLs utilizing alternative SA materials, as outlined in table 1. The comparison highlights that the PAN-based SA demonstrates performance on par with other materials. We anticipate that further optimization of both the fibre cavity and SA parameters could lead to enhanced Q-switching performance. Compared to alternative materials like graphene, CNTs, emerging 2D materials, and rare earth materials, Polyacrylonitrile SA offers several collective advantages. These include robust resistance to [illegible] a broad absorption spectrum, and

suitable modulation depth. However, it's important to note that they may exhibit a lower optical damage threshold when compared to ceramic materials such as MAX phases and MXene materials.

Conclusion

A straightforward and robust Q-switched EDFL is presented utilizing a PAN-based SA, formed by embedding PAN compounds onto a PVA host. Operating at 1572 nm, the EDFL exhibits stability across a pump power range of 113.3 to 175.9 mW. Notably, as pump power increases, both repetition rate and pulse energy of the EDFL escalate, while pulse width diminishes. Employing the PAN SA, the EDFL attains peak performance metrics, including a maximum pulse energy of 52 nJ, highest repetition rate of 66.1 kHz, and lowest pulse width of 2.43 μs. These results underscore the potential of PAN for laser applications, particularly within the L-band wavelength range. Furthermore, the proposed EDFL offers simplicity, cost-effectiveness, and suitability for diverse applications such as metrology, environmental sensing, and biomedical diagnostics.

Acknowledgments

This work is supported by the Malaysian Ministry of Higher Education under fundamental research grant scheme (Grant No: FRGS/1/2022/TK07/UM/02/34).

Data availability statement

All data that support the findings of this study are included within the article (and any supplementary files).

ORCID iDs

Sameer Salam https://orcid.org/0000-0001-5056-5315
Sulaiman W Harun https://orcid.org/0000-0003-4879-5853

References

[1] Leone C, Papa I, Tagliaferri F and Lopresto V 2013 Investigation of CFRP laser milling using a 30 W Q-switched Yb: YAG fiber laser: Effect of process parameters on removal mechanisms and HAZ formation *CompoSiteS Part a: applied science and manufacturing* **55** 129–42
[2] Weissleder R and Nahrendorf M 2015 Advancing biomedical imaging *Proc. Natl Acad. Sci.* **112** 14424–8
[3] Skorczakowski M *et al* 2010 'Mid-infrared Q-switched Er: YAG laser for medical applications, *Laser Phys. Lett.* **7** 498
[4] Li Z *et al* 2013 Diode-pumped wideband thulium-doped fiber amplifiers for optical communications in the 1800–2050 nm window *Opt. Express* **21** 26450–5
[5] Rung S, Häcker N and Hellmann R 2022 Micromachining of alumina using a high-power ultrashort-pulsed laser *Materials* **15** 5328
[6] Chaudhary R, Fabbri P, Leoni E, Mazzanti F, Akbari R and Antonini C 2023 Additive manufacturing by digital light processing: a review *Progress in Additive Manufacturing* **8** 331–51
[7] Chen X, Wang N, He C and Lin X 2023 Development of all-fiber nanosecond oscillator using actively Q-switched technologies and modulators *Opt. Laser Technol.* **157** 108709
[8] Saunders J, Elbestawi M and Fang Q 2023 Ultrafast laser additive manufacturing: a review *Journal of Manufacturing and Materials Processing* **7** 89
[9] Qamar F 2005 *Mid-IR Fibre Lasers: Continuous, Pulsed and Self Dynamical Characteristics* (The University of Manchester)
[10] Tang C Y 2020 Optical nonlinear properties of novel two dimensional transition metal dichalcogenides *PhD thesis* The Hong Kong Polytechnic University
[11] Weiner A M 2000 'Femtosecond pulse shaping using spatial light modulators, *Rev. Sci. Instrum.* **71** 1929–60
[12] Hong H, Huang L, Liu Q, Yan P and Gong M 2012 Compact high-power, TEM 00 acousto-optics Q-switched Nd: YVO 4 oscillator pumped at 888 nm *Appl. Opt.* **51** 323–7
[13] Wang Y *et al* 2019 An all-optical, actively Q-switched fiber laser by an antimonene-based optical modulator *Laser Photonics Rev.* **13** 1800313
[14] Ji J, Zhu X, Dai S and Wang C 2007 Depolarization loss compensated resonator for electro-optic Q-switched solid-state laser *Opt. Commun.* **270** 301–4
[15] Lee J, Jung M, Koo J, Chi C and Lee J H 2014 Passively Q-switched 1.89-μm fiber laser using a bulk-structured Bi 2 Te 3 topological insulator *IEEE J. Sel. Top. Quantum Electron.* **21** 31–6
[16] Lee J, Koo J, Chi C and Lee J H 2014 'All-fiberized, passively Q-switched 1.06 μm laser using a bulk-structured Bi2Te3 topological insulator, *J. Opt.* **16** 085203
[17] Lu L *et al* 2018 'Few-layer bismuthene: sonochemical exfoliation, nonlinear optics and applications for ultrafast photonics with enhanced stability, *Laser Photonics Rev.* **12** 1700221
[18] Lau K, Ker P J, Abas A, Alresheedi M and Mahdi M 2019 Long-term stability and sustainability evaluation for mode-locked fiber laser with graphene/PMMA saturable absorbers *Opt. Commun.* **435** 251–4
[19] Haoken A V, Diblawe A M and Harun S W 2023 'Enhanced Q-switched pu[illegible]n at 1.5 μm in erbium-doped fiber laser using thin-film dititanium tin carbide as a saturable absorber, *Results in Optics* **1**[illegible]

[20] Chen Y, Cheak T Z, Jin T S, Vinitha G, Dimyati K and Harun S W 2024 Domain-wall dark pulse generation with SMF-GIMF-SMF structure as artificial saturable absorber *Sci. Rep.* **14** 2141
[21] Hamzah A *et al* 2013 'Passively mode-locked erbium doped zirconia fiber laser using a nonlinear polarisation rotation technique, *Opt. Laser Technol.* **47** 22–5
[22] Xu Z, Dou Z-Y, Hou J and Xu X-J 2017 All-fiber wavelength-tunable Tm-doped fiber laser mode locked by SESAM with 120 nm tuning range *Appl. Opt.* **56** 5978–81
[23] Sun Z *et al* 2010 Graphene mode-locked ultrafast laser *ACS nano* **4** 803–10
[24] Ismail M, Ahmad F, Harun S W, Arof H and Ahmad H 2013 'A Q-switched erbium-doped fiber laser with a graphene saturable absorber, *Laser Phys. Lett.* **10** 025102
[25] Meng Y, Li Y, Xu Y and Wang F 2017 Carbon nanotube mode-locked thulium fiber laser with 200 nm tuning range *Sci. Rep.* **7** 45109
[26] Fang Q, Kieu K and Peyghambarian N 2010 An all-fiber 2 μm wavelength-tunable mode-locked laser *IEEE Photonics Technol. Lett.* **22** 1656–8
[27] Jung M *et al* 2014 A femtosecond pulse fiber laser at 1935 nm using a bulk-structured Bi 2 Te 3 topological insulator *Opt. Express* **22** 7865–74
[28] Lin Y-H *et al* 2015 Using n-and p-type Bi2Te3 topological insulator nanoparticles to enable controlled femtosecond mode-locking of fiber lasers *Acs Photonics* **2** 481–90
[29] Qin Z, Xie G, Zhao C, Wen S, Yuan P and Qian L 2016 Mid-infrared mode-locked pulse generation with multilayer black phosphorus as saturable absorber *Opt. Lett.* **41** 56–9
[30] Sotor J, Sobon G, Kowalczyk M, Macherzynski W, Paletko P and Abramski K M 2015 Ultrafast thulium-doped fiber laser mode locked with black phosphorus *Opt. Lett.* **40** 3885–8
[31] Zhu X, Wang J, Lau P, Nguyen D, Norwood R and Peyghambarian N 2010 Nonlinear optical performance of periodic structures made from composites of polymers and Co3O4 nanoparticles *Appl. Phys. Lett.* **97** 093503
[32] Mamani J B, Gamarra L F and Brito G E d S 2014 Synthesis and characterization of Fe3O4 nanoparticles with perspectives in biomedical applications *Mater. Res.* **17** 542–9
[33] Wu K, Zhang X, Wang J, Li X and Chen J 2015 WS 2 as a saturable absorber for ultrafast photonic applications of mode-locked and Q-switched lasers *Opt. Express* **23** 11453–61
[34] Wiles K B 2002 *Determination of Reactivity Ratios For Acrylonitrile/Methyl Acrylate Radical Copolymerization Via Nonlinear Methodologies Using Real Time FTIR* (Virginia Tech)
[35] Fitzer E 1989 Pan-based carbon fibers—present state and trend of the technology from the viewpoint of possibilities and limits to influence and to control the fiber properties by the process parameters *Carbon* **27** 621–45
[36] Chen J and Harrison I 2002 Modification of polyacrylonitrile (PAN) carbon fiber precursor via post-spinning plasticization and stretching in dimethyl formamide (DMF) *Carbon* **40** 25–45
[37] Rahaman M S A, Ismail A F and Mustafa A 2007 'A review of heat treatment on polyacrylonitrile fiber, *Polym. Degrad. Stab.* **92** 1421–32
[38] Hader J, Yang H-J, Scheller M, Moloney J V and Koch S W 2016 Microscopic analysis of saturable absorbers: Semiconductor saturable absorber mirrors versus graphene *J. Appl. Phys.* **119** 053102
[39] Qi Y *et al* 2022 'Tunable all fiber multi-wavelength mode-locked laser with a large dynamic range using polarization controller coiled SMF-GIMF-SMF structure as both saturable absorber and comb filter, *Opt. Fiber Technol.* **74** 103055
[40] Zheng Z *et al* 2012 Microwave and optical saturable absorption in graphene *Opt. Express* **20** 23201–14
[41] Popa D, Sun Z, Hasan T, Torrisi F, Wang F and Ferrari A 2011 Graphene Q-switched, tunable fiber laser *Appl. Phys. Lett.* **98** 073106
[42] Lee J, Lee J, Koo J, Chung H and Lee J H 2016 Linearly polarized, Q-switched, erbium-doped fiber laser incorporating a bulk-structured bismuth telluride/polyvinyl alcohol saturable absorber *Opt. Eng.* **55** 076109
[43] Chen Y *et al* 2015 'Mechanically exfoliated black phosphorus as a new saturable absorber for both Q-switching and mode-locking laser operation, *Opt. Express* **23** 12823–33
[44] Ahmad M T *et al* 2019 Q-switched Ytterbium doped fibre laser using gold nanoparticles saturable absorber fabricated by electron beam deposition *Optik* **182** 241–8
[45] Li L *et al* 2018 Transition metal dichalcogenide (WS2 and MoS2) saturable absorbers for Q-switched Er-doped fiber lasers *Laser Phys.* **28** 055106
[46] Haris H *et al* 2019 Passively Q-switched and mode-locked erbium-doped fiber laser with topological insulator Bismuth Selenide (Bi2Se3) as saturable absorber at C-band region *Opt. Fiber Technol.* **48** 117–22
[47] Ghafar N A M, Zulkipli N F, Omar S, Markom A M, Yasin M and Harun S W 2022 Q-Switched Pulse generation in erbium-doped fiber laser cavity with vanadium aluminum carbide absorber *J. Russ. Laser Res.* **43** 702–7
[48] Diblawe A M *et al* 2023 Molybdenum aluminum boride as the Q-Switcher and Mode-locker in the erbium-doped fiber laser configuration *J. Russ. Laser Res.* **44** 68–76